Available online at www.sciencedirect.com
SCIENCE DIRECT
Journal of Solid State Chemistry 177 (2004) 4399–4403
JOURNAL OF SOLID STATE CHEMISTRY
www.elsevier.com/locate/jssc

A simple method to synthesize single-crystalline lanthanide orthovanadate nanorods

Weiliu Fan[a], Wei Zhao[a], Liping You[b], Xinyu Song[a], Weimin Zhang[a], Haiyun Yu[a], Sixiu Sun[a,*]

[a]*The School and Department of Chemistry, Shandong University, Jinan City, Shandong Province 250100, PR China*
[b]*Electron Microscopy Laboratory, Peking University, Beijing, 100871, PR China*

Received 16 June 2004; received in revised form 6 August 2004; accepted 16 August 2004
Available online 11 November 2004

Abstract

Single-crystalline tetragonal $LnVO_4$ (Ln = La, Nd, Sm, Eu, Dy) nanorods were prepared via a simple hydrothermal method, in the absence of any surfactant or template using cheap and simple inorganic salts as raw materials. The products were characterized by XRD, TEM, HRTEM, and PL. It has been shown that after the hydrothermal process, $LaVO_4$ transformed its crystal structure from monoclinic to tetragonal phase, but $LnVO_4$ (Ln = Nd, Sm, Eu, Dy) have not exhibited the structural change. This could be associated with the change of lanthanide ion radius. TEM and HRTEM results show that the nanorods are pure, structurally uniform, single crystalline, and most of them are free from dislocations. Further study reveals the nanorods grow along the [001] direction. A possible growth mechanism of lanthanide orthovanadate nanorods was also proposed. The advantages of our method for the nanorods synthesis lie in the high yield and the low temperature and mild reaction conditions, which permit large scale production at low cost.
© 2004 Elsevier Inc. All rights reserved.

Keywords: Lanthanide orthovanadate; Nanorods; Hydrothermal; Oswald ripening

1. Introduction

Nanostructured materials are expected to play a crucial role in the future technological advance in electronics [1], optoelectronics [2], and memory devices [3]. One-dimensional (1D) nanostructures, such as nanorods or nanowires, in particular offer fundamental opportunities for investigating the effect of size and dimensionality on their collective optical, magnetic, and electronic properties [4–6].

Although a number of synthetic methodologies have been developed to fabricate and assemble 1D nanostructures [7], they often suffer from the requirements of high temperature, special conditions, tedious procedures, and catalyst or templates. Therefore, the development of practical methods for fabricating large numbers of 1D nanostructures at low cost is still a great challenge for future study. Chemical methods, on the other hand, seem to provide an alternative and intriguing strategy for generating 1D nanostructures with respect to material diversity, cost, versatility, synthetic tenability, and potential for large scale production, of the methods employed in the synthesis of 1D nanomaterials, hydrothermal methods have been regarded as effective routes to the fabrication of high-quality anisotropic nanomaterials [7a,8]. Several solution-phase procedures have been demonstrated for generating 1D nanostructures [9].

Because of their unique electronic structure and the numerous transition modes involving the 4*f* shell of their ions, lanthanide compounds usually have outstanding optical, electrical, and magnetic properties, and have been widely used [10]. There have been extensive studies

---

*Corresponding author. Fax: +86-561-856-4464.
E-mail address: ssx@sdu.edu.cn (S. Sun).

0022-4596/$ - see front matter © 2004 Elsevier Inc. All rights reserved.
doi:10.1016/j.jssc.2004.08.027

regarding lanthanide chemistry at bulk or atomic levels, and more recently, some work have been reported on the synthesis of rare earth compound nanotubes and nanowires/nanorods by hydrothermal processes [7a, 11].

Single crystals of rare earth orthovanadates have been expected to be attractive materials for various applications such as an efficient phosphor, a low-threshold laser host and a polarizer material. To obtain the high quality of lanthanide and related orthovanadate crystals, several methods such as Floating Zone method, Czochralski method, flux method and top-seeded solution growth (TSSG) method have been carried out [12]. However, to the best of our knowledge, previously there have been no studies focused on the synthesis of nanorods or nanowires of lanthanide orthovanadate (LnVO$_4$). Herein, we report the systematic synthesis of high-quality LnVO$_4$ single-crystal nanorods through a facile solution-based hydrothermal synthetic pathway. A possible growth mechanism of the nanorods is also presented here. This would be of great significance because of the possible novel properties induced by the reduced dimensionality.

2. Experimental

2.1. Preparation of the $LnVO_4$ nanorods

Analytical grade lanthanide nitrate and NaVO$_3$ were purchased from the Shanghai chemical industrial company and were used without further purification. The tetragonal LnVO$_4$ (Ln = La, Nd, Sm, Eu, Dy) nanorods were prepared by a simple hydrothermal method. The reaction was carried out in a 20 mL capacity Teflon-lined stainless-steel autoclave, in a digital-type temperature-controlled oven. Taking the synthesis of LaVO$_4$ as example, in a typical synthesis 16 mL of NaVO$_3$ (0.2 M) aqueous solution were added into 8 mL of La(NO$_3$)$_3$ aqueous solution (0.4 M) at room temperature under vigorous stirring, the solution turned yellow immediately after the addition of the NaVO$_3$. The obtained yellow suspension was stirred for about 10 min, then 4.8 mL 1 M NaOH aqueous solution was added to adjust the pH to 4.5. The resulting yellow suspension was divided into two equal parts. The first half was filtered off, washed with distilled water and absolute ethanol, respectively, and then dried at room temperature under vacuum overnight for further characterization. The product appeared as yellow prismatic crystals, which were identified as monoclinic LaVO$_4$ by X-ray diffractometry. The second was poured into a Teflon-lined stainless-steel autoclave. The autoclave was sealed and maintained at 180 °C for 48 h and then air cooled to room temperature, the resulting LnVO$_4$ products were filtered, washed with deionized water and absolute alcohol to remove ions possibly remaining in the final products, and finally dried at 80°C in air for further characterization, the products (tetragonal LaVO$_4$) obtained after hydrothermal process were white powders.

Under the same hydrothermal process, tetragonal phase LnVO$_4$ (Ln = Nd, Sm, Eu, Dy) nanorods were also prepared with the pH adjusted to a specific value (pH = 4.5–5.5) using 1 M NaOH aqueous solution. Main products of the present system were white powders, expect that the NdVO$_4$ was silver gray.

2.2. Characterization

The phase purity of the product was examined by X-ray diffraction (XRD) using a Japan Rigaku D/Max-γA rotation anode X-ray diffractometer equipped with graphite monochromatized Cu$K\alpha$ radiation ($\lambda = 1.54178$ Å), employing a scanning rate of $0.02^\circ\,\text{s}^{-1}$ in the 2θ range from 10° to 75°. The operation voltage and current were maintained at 40 kV and 40 mA, respectively. The morphologies and micro- and nanostructure of the as-synthesized LnVO$_4$ products were characterized by transmission electron microscopy (TEM), carried out using JEOL JEM-100 CX II at an accelerating voltage of 100 KV. Further structural characterization was performed on a Philips Tecnai F30 high-resolution field-emission transmission electron microscope (HRTEM) operating at 300 kV. The samples for these measurements were dispersed in absolute ethanol by being vibrated in the ultrasonic pool. Then, the solutions were dropped onto a copper grid coated with amorphous carbon films and dried in air before performance. Room-temperature photoluminescence (PL) spectra were recorded by a Hitachi 850 fluorescence spectrometer with a Xe lamp as the excitation source at 25°C.

3. Results and discussion

X-ray diffraction (XRD) has been used to characterize the crystal structure change of the LaVO$_4$ pre- and post-reaction with hydrothermal. Fig. 1a shows a typical XRD pattern of LaVO$_4$ as-prepared without hydrothermal process, and all the peaks could be readily indexed to a monoclinic phase with lattice constants comparable with the values given in JCPDS (25-0427). The XRD pattern of LaVO$_4$ nanorods prepared through the facile hydrothermal method is displayed in Fig. 1b, and most of the peaks could be indexed to a tetragonal structure for bulk LaVO$_4$: space group $I4_1/amd$ with cell constants $a = 7.50$ and $c = 6.59$ Å (JCPDS Card number: 32-0504).

The morphology and structure details of the products were further characterized by transmission electron microscopy (TEM) and high-resolution field-emission

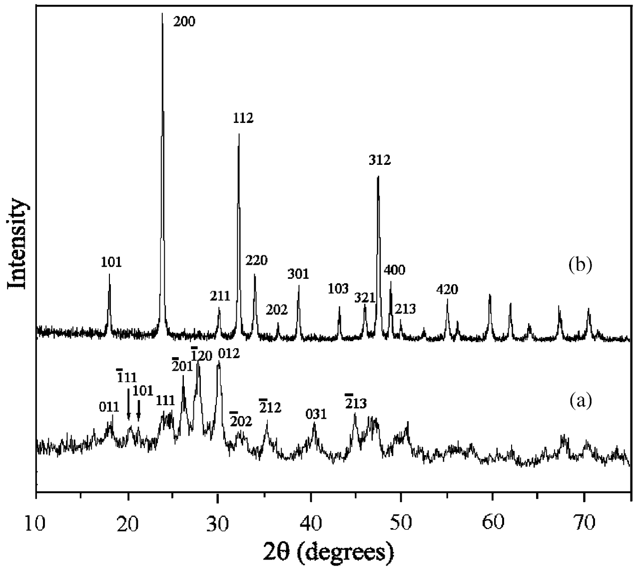

Fig. 1. XRD pattern of the $LaVO_4$ particles obtained (a) before (b) after hydrothermal treatment at 180 °C for 48 h with pH 4.5.

TEM (HRTEM) combined with a fast two-dimensional Fourier transform (FFT) analysis technique. Fig. 2a gives a typical TEM image of the $LaVO_4$ product obtained before hydrothermal treatment. The monoclinic $LaVO_4$ colloidal precipitates were irregular particles and aggregates with size around 10–30 nm. Those nanoparticles could serve as anisotropic seeds for the growth of highly anisotropic 1D nanostructures in the solution solid process via the dissolution and crystallization mechanism in present case. Fig. 2b, a typical TEM image of the $LaVO_4$ product, as-obtained after hydrothermal treatment at 180°C for 48 h with pH at 4.5, clearly reveals a rod-like morphology with average diameters of 20 nm and lengths of up to 100 nm. The HRTEM image (Fig. 2c) shows that the nanorods are structurally uniform, and are free from defects and dislocations. The lattice spacings of about 0.374 and 0.659 nm correspond to the (200) plane and the *c*-axis of a unit cell tetragonal phase $LaVO_4$, respectively. Fig. 2d is a FFT of the HRTEM image. From the examination of the spatial arrangement of the spots in the FFT pattern, it was found that the set of lattice planes giving rise to all these spots derives from a single tetragonal crystal with its [010] direction being oriented toward the direction of the electron beam. In other words, the FFT pattern of Fig. 2d corresponds to the diffraction pattern with a [010] zone axis. Further studies of the HRTEM image and FFT pattern demonstrate that the direction of nanorod growth is along the *c*-axis, i.e. the [001] direction (indicated with an arrow).

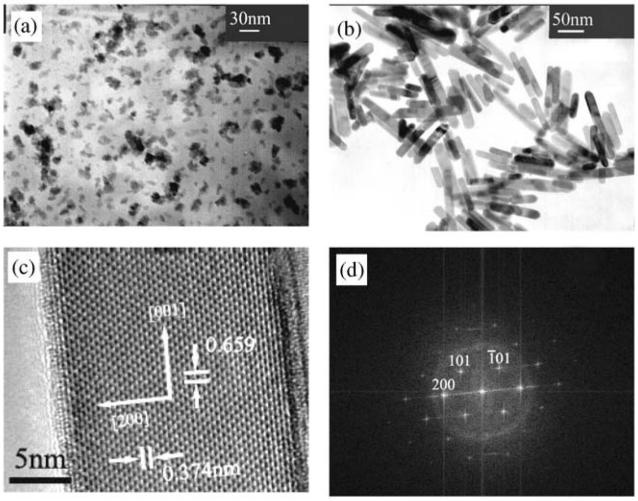

Fig. 2. Typical TEM images of the as-synthesized $LaVO_4$ (a) before hydrothermal treatment (b) after hydrothermal treatment, showing the change in morphology. (c) HRTEM image taken on a single nanorod with diameter of about 20 nm showing clear lattice fringes of about 0.374 nm and 0.659 nm corresponding to (200) plane and the *c*-axis of a unit cell, respectively. (c) Corresponding fast two-dimensional Fourier transform (FFT) of the HRTEM image.

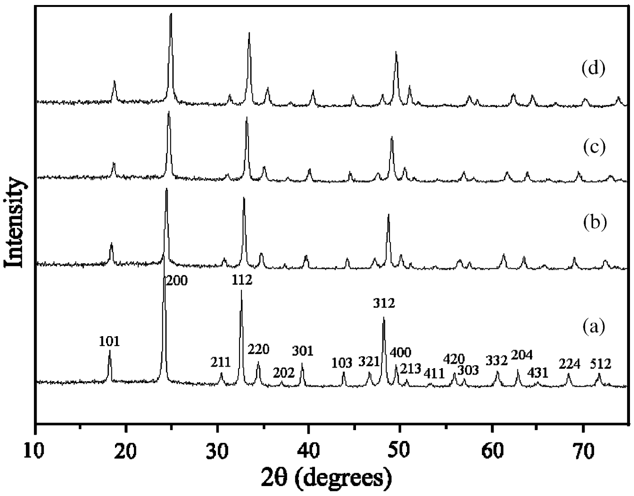

Fig. 3. XRD pattern of the as-synthesized lanthanide orthovanadate nanorods. (a) $NdVO_4$, (b) $SmVO_4$, (c) $EuVO_4$ and (d) $DyVO_4$. All products were obtained after hydrothermal treatment at 180°C for 48 h with proper pH.

Through the similar hydrothermal process with controlled proper pH, other lanthanide orthovanadate $LnVO_4$ (Ln = Nd, Sm, Eu, Dy) nanorods have also been synthesized. The XRD patterns of the products are shown in Fig. 3. All reflection peaks of the as-synthesized different products can be easily indexed as a pure, tetragonal zircon-type $LnVO_4$ structure with cell parameters $NdVO_4$: $a = 7.335$ Å, $c = 6.431$ Å; $SmVO_4$: $a = 7.265$ Å, $c = 6.389$ Å; $EuVO_4$: $a = 7.236$ Å, $c = 6.367$ Å; $DyVO_4$: $a = 7.140$ Å, $c = 6.311$ Å, which are in good agreement with literature values (JCPDS Card number: 72-0280, 17-0876, 15-0809, 71-0845). As we can see from the patterns, with decreasing ion radius, the peaks in the tetragonal phase gradually shift to smaller *d* values. On the other hand, during the synthesis of LnVO$_4$ (Ln = Nd, Sm, Eu, Dy), we have found no structural change from monoclinic to tetragonal phase; these vanadates only have a tetragonal structure pre- and post-hydrothermal treatment (XRD patterns of the products obtained without hydrothermal treatment were shown in Fig. S1, supporting information).

Why does LaVO$_4$ have a crystal phase transformation from monoclinic structure to tetragonal structure, but LnVO$_4$ (Ln = Nd, Sm, Eu, Dy) have not? It is believed that this could be associated with the change of lanthanide ion radius. The orthovanadate crystallizes in two types, namely, monoclinic monazite (CePO$_4$) type and tetragonal zircon (ZrSiO$_4$) type. Generally the larger Ln^{3+} ion prefers the monazite type due to its higher oxygen coordination number of 9 as compared to 8 of the zircon type, and it is interesting to note that CeVO$_4$ locating in the boundary of zircon and monazite types [13]. So, in the case of LaVO$_4$, the tetragonal structure is a metastable phase. In order to obtain metastable phases, solution processes sometimes work well. In our report, using a facile hydrothermal method we successfully synthesized tetragonal LaVO$_4$ in high crystallinity with nanorod morphology.

Figs. 4a–d display the typical TEM images of tetragonal LnVO$_4$ (Ln = Nd, Sm, Eu, Dy) nanorods, respectively. From the images we can see, the as-synthesized LnVO$_4$ products consist almost entirely of nanorods with diameters of 10–50 nm and lengths of 50–200 nm. The high density of nanorods is representative of the high yields associated with this facile preparation approach. The morphology of LnVO$_4$ (Ln = Nd, Sm, Eu, Dy) as-obtained before hydrothermal treatment can be investigated from Fig. S2, supporting information.

Fluorescence spectroscopy can provide valuable information about the intermolecular interactions of molecules in molecular crystals and monolayers [14]. Room-temperature photoluminescence (PL) spectra of the as-synthesized LaVO$_4$ monoclinic nanoparticles and tetragonal nanorods were measured with excitation wavelengths of 280 and 318 nm, respectively, under identical experiment conditions. As show in Fig. 5a, two very weak emissions, peaking at 369 nm (3.36 eV) and 459 nm (2.70 eV), were observed for the monoclinic LaVO$_4$ nanoparticles. Fig. 5b shows the fluorescence spectrum of the tetragonal LaVO$_4$ nanorods, an intense emission centered at 428 nm (2.90 eV) and a marked sharp shoulder with an emission maximum at 515 nm (2.40 eV) are visible. Compared to the PL emission of monoclinic LaVO$_4$ nanoparticles, the PL emission is red shifted by about 59 nm, which may be caused by the oriented growth of the nanocrystallites of the tetragonal LaVO$_4$ nanorods [15]. The determination of the detailed optical properties of the LaVO$_4$ and other lanthanide orthovanadate nanorods is still underway.

Although the detail study of growth mechanism of the nanorods is in progress, we believe that the growth of the nanorods is not catalyst-assisted or template-directed, because no additional catalysts or templates were introduced into the reaction. Based on the observation of TEM images, we proposed that the process of crystal growth and morphology evolution might mainly be fabricated by an Ostwald ripening: a highly supersaturated solution was adopted and irregular fine particles acted as the precursor for the synthesis of crystallized LnVO$_4$ nanorods. The formation of tiny crystalline nuclei in a supersaturated medium occurred at first, and this was followed by crystal growth. The larger particles grew at the cost of the small particles; reduction in surface energy is the primary driving force for crystal growth and morphology evolution, due to the difference in solubility between the larger particles and

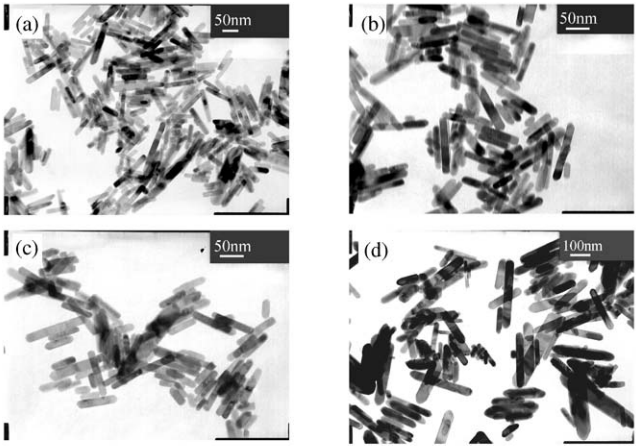

Fig. 4. Typical TEM images of as-synthesized nanorods. (a) NdVO$_4$, (b) SmVO$_4$, (c) EuVO$_4$ and (d) DyVO$_4$ obtained after hydrothermal treatment at 180°C for 48 h with proper pH.

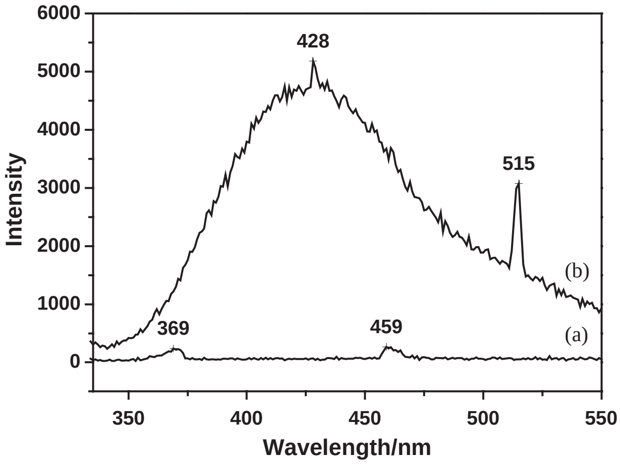

Fig. 5. Room-temperature photoluminescence spectra of (a) monoclinic LaVO$_4$ nanoparticles as-synthesized before hydrothermal process and (b) tetragonal LaVO$_4$ nanorods obtained after the hydrothermal treatment.

the small particles, according to the well-known Gibbs–Thomson law. As the reaction continued, the irregular nanoparticles vanished and longer nanorods formed [8b, 16]. When Ostwald ripening is the dominant mechanism of the nanorods growth, the formation of the nanorods must be affected by the character of the starting materials, such as, the particle size and/or chemical activity because the dissolution rate of the material depend on such characters. Further study suggests that the process is strongly dependent on the experimental details (pH, concentration, temperature).

4. Conclusions

In summary, we have found a simple route to prepare single-crystal tetragonal $Ln\mathrm{VO}_4$ (Ln = La, Nd, Sm, Eu, Dy) nanorods by facile hydrothermal treatment and the growth mechanism is also discussed. The simplicity of hydrothermal process, cheapness, and availability of raw materials are advantages favoring the scaling-up of nanorods. We think the present study has enlarged the family of 1D nanostructures of rare earth compounds, and the availability of $Ln\mathrm{VO}_4$ nanostructures with low dimensionalities should be able to bring in new types of applications or to enhance the performance of the currently existing devices as a result of quantum-sized effects. Further work is under way to explore the more evidence about the formation mechanism, properties of this novel nanorods, and the possibility of synthesizing other lanthanide vanadate nanorods.

References

[1] Y. Cui, C.M. Liber, Science 291 (2001) 851.
[2] A.P. Alivisatos, Science 271 (1996) 933.
[3] S. Sun, C.B. Murray, D. Weller, L. Folks, A. Moser, Science 287 (2000) 1989.
[4] J. Hu, T.W. Odom, C.M. Liber, Acc. Chem. Res. 32 (1999) 435.
[5] Y.N. Xia, P.D. Yang, Y. Wu, B. Mayers, B. Gates, Y. Yin, F. Kim, H. Yan, Adv. Mater. 15 (2003) 353.
[6] M.H. Huang, S. Mao, H. Feick, H.Q. Yan, Y.Y. Wu, H. Kind, E. Weber, R. Russo, P.D. Yang, Science 292 (2001) 1897.
[7] (a) Y.P. Fang, A.W. Xu, R.Q. Song, H.X. Zhang, L.P. You, J.C. Yu, H.Q. Liu, J. Am. Chem. Soc. 125 (2003) 16025;
(b) M. Brorson, T.W. Hansen, C.J.H. Jacobsen, J. Am. Chem. Soc. 124 (2002) 11582;
(c) P.M. Ajayan, O. Stephan, P. Redlich, C. Colliex, Nature 375 (1995) 564.
[8] (a) G.R. Patzke, F. Krumeich, R. Nesper, Angew. Chem. Int. Ed. 41 (2002) 2446;
(b) S.H. Yu, L. Biao, M.S. Mo, J.H. Huang, X.M. Liu, Y.T. Qian, Adv. Funct. Mater 13 (2003) 639;
(c) X. Wang, Y.D. Li, Chem. Eur. J. 9 (2003) 300.
[9] (a) J.D. Holmes, K.P. Johnston, R.C. Doty, B.A. Korgel, Science 287 (2000) 1471;
(b) L. Vayssieres, Adv. Mater. 15 (2003) 464.
[10] (a) J.P. Cotter, J.C. Fitzmaurice, I.P. Parkin, J. Mater. Chem. 4 (1994) 1603;
(b) M.S. Palmer, M. Neurock, M.M. Olken, J. Am. Chem. Soc. 124 (2002) 8452;
(c) R. Kempe, H. Noss, T. Irrgang, J. Organomet. Chem. 647 (2002) 12;
(d) J.W. Stouwdam, F.C.J.M. van Veggel, Nano Lett. 2 (2002) 733.
[11] (a) X. Wang, Y.D. Li, Angew. Chem. Int. Ed. 41 (2002) 4790;
(b) X. Wang, Y.D. Li, Chem. Eur. J. 9 (2003) 5627;
(c) X. Wang, X.M. Sun, D.P. Yu, B.S. Zou, Y.D. Li, Adv. Mater. 15 (2003) 1442;
(d) A.W. Xu, Y.P. Fang, L.P. You, H.Q. Liu, J. Am. Chem. Soc. 125 (2003) 1494.
[12] (a) Y. Terada, T. Maeda, V.V. Kochurikhin, K. Shimamura, S. Uda, T. Fukuda, J. Cryst. Growth 178 (1997) 518;
(b) M. Kawasaki, T. Katsumata, Y. Oshiba, M. Koshiji, J. Cryst. Growth 198/199 (1999) 449;
(c) K. Shimamura, S. Uda, V.V. Kochurikhin, T. Taniuchi, T. Fukuda, Jpn. J. Appl. Phys. 35 (1996) 320;
(d) B.C. Chakoumakos, M.M. Abraham, L.A. Boatner, J. Solid. State. Chem. 109 (1994) 197;
(e) D.F. Mullica, E.L. Sappenfield, M.M. Abraham, B.C. Chakoumaskos, Inorg. Chim. Acta 248 (1996) 88;
(f) S. Varma, B.N. Wani, N.M. Gupta, Mater. Res. Bull. 37 (2002) 2117.
[13] (a) H. Fuess, A. Kallel, J. Solid State Chem. 5 (1972) 11;
(b) B.C. Chakoumakos, M.M. Abraham, L.A. Boatner, J. Solid. State Chem. 109 (1994) 197;
(c) Y. Oka, T. Yao, N. Yamamoto, J. Solid. State Chem. 152 (2000) 486.
[14] Y. Hu, J.F. Chen, W.M. Chen, X.H. Lin, X.L. Li, Adv. Mater. 15 (2003) 726.
[15] H.W. Liao, Y.F. Wang, X.M. Liu, Y.D. Li, Y.T. Qian, Chem. Mater. 12 (2000) 2819.
[16] J.W. Mullin, Crystallization, 3rd ed, Butterworth-Heinemann, Oxford, 1997.